A reconstructed South Atlantic Meridional Overturning Circulation time series since 1870

Hosmay Lopez[1,2], Gustavo Goni[2] and Shenfu Dong[2].
[1] CIMAS, University of Miami, Miami, FL, USA, [2] Atlantic Oceanographic and Meteorological Laboratory, NOAA, Miami, FL, USA
Contact info : Hosmay.Lopez@noaa.gov

Introduction

Recently, the research community started investigating the role of the South Atlantic on climate. The AMOC over the South Atlantic is unique given that it is the only major ocean basin that transports heat equatorward (Talley 2003). Recent studies suggests the possibility of the anomalous AMOC originating from inter-ocean transport from the Indian Ocean (Lee et al. 2011) with large repercussions on the global monsoon precipitation system (Lopez et al. 2016a).

This study reconstructs a century-long South Atlantic Meridional Overturning Circulation (SAMOC) index. The reconstruction is possible due to its co-variability with sea surface temperature (SST). A singular value decomposition (SVD) method is applied to the correlation matrix of SST and SAMOC. The SVD is performed on the trained period (1993-present) for which Expendable Bathythermographs (XBT) and satellite altimetry observations of the SAMOC are available. The joint modes obtained are used in the reconstruction of a monthly SAMOC time series $\hat{y}$ using SST $x(t)$ from 1870 to present:

$$\hat{y}(t) = \sum_{k=1}^{q} \frac{cov(a_k, b_k)}{var(a_k)} \boldsymbol{U}_k^T x(t) \boldsymbol{V}_k , \qquad q = 4, t = 1870{:}\,2016$$

where $\boldsymbol{U}$ is a matrix, whose columns contain the singular vectors of SST, and $\boldsymbol{V}$ is a matrix, which rows contain the singular vectors of SAMOC. The vectors a_k and b_k are the expansion coefficients for SST and SAMOC respectively.

Key Results:

- A century-long reconstructed South Atlantic Meridional Overturning Circulation index at four latitudes from sea surface temperature is presented.
- The Inter-decadal Pacific Oscillation (IPO) is the leading mode of SAMOC-SST co-variability, explaining ~85% with the Atlantic Niño accounting for less than 10% (Lopez et al. 2016b). **(Fig. 1).**
- The reconstructed index is highly correlated to the observational-based SAMOC time series during the trained period and provides a long historical estimate. **(Figs. 2 and 3).**
- SAMOC has recently shifted to an anomalous positive period (Lopez et al. 2017), consistent with a recent positive shift of the IPO (Burgman et al. 2016). **(Fig. 2).**
- The meridional coherence is similar between the observed and reconstructed SAMOC. **(Fig. 4).**
- SAMOC could serve as a predictor of decadal monsoon variability with 20-year lead-time (Lopez et al. 2016a). **(Figs. 5, 6 and 7).**

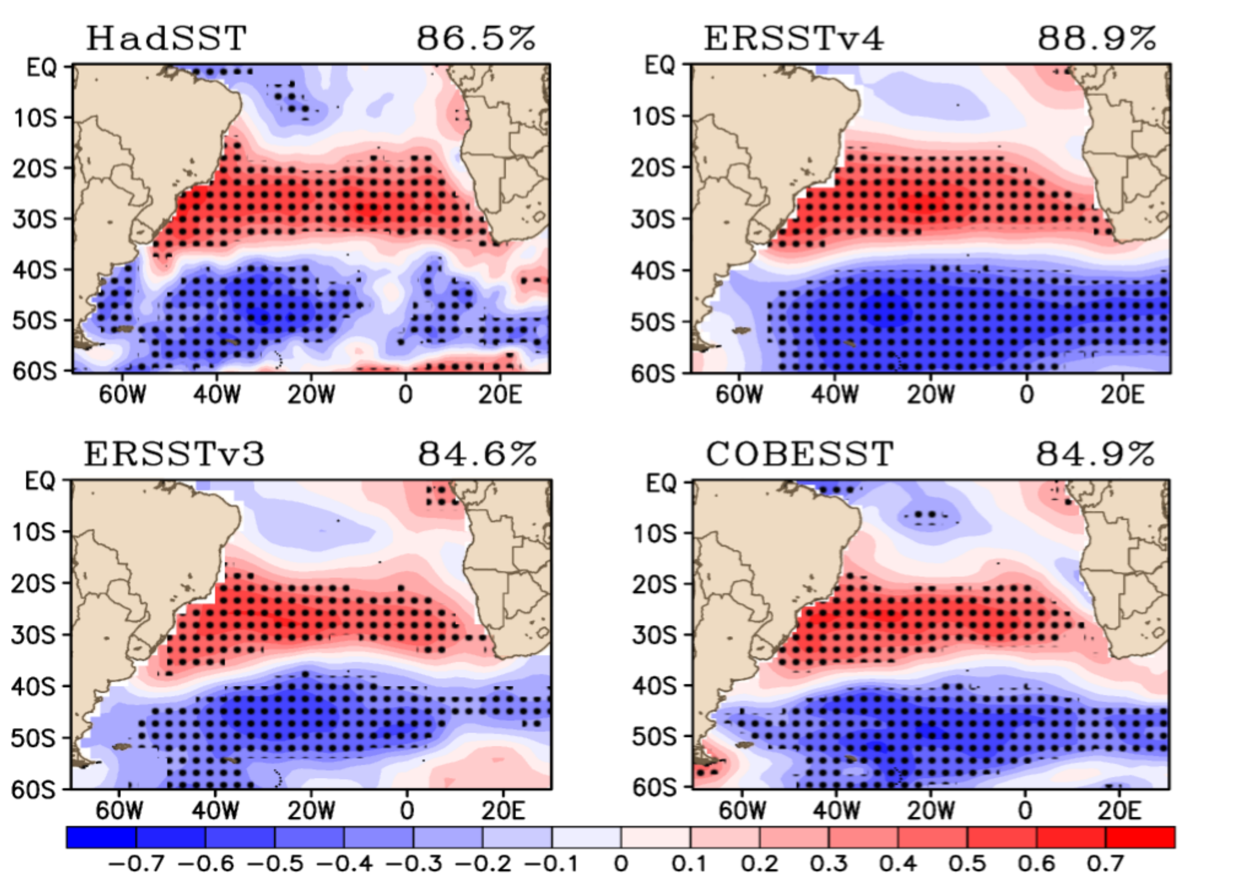

Figure 1. Heterogeneous correlation for the first joint singular vector from the observed SAMOC SST covariance matrix for each SST product. Black hatching indicates where the heterogeneous correlation is significant at a 95% confidence level. The percentage on the top right indicates the amount of co-variance explained by the first mode.

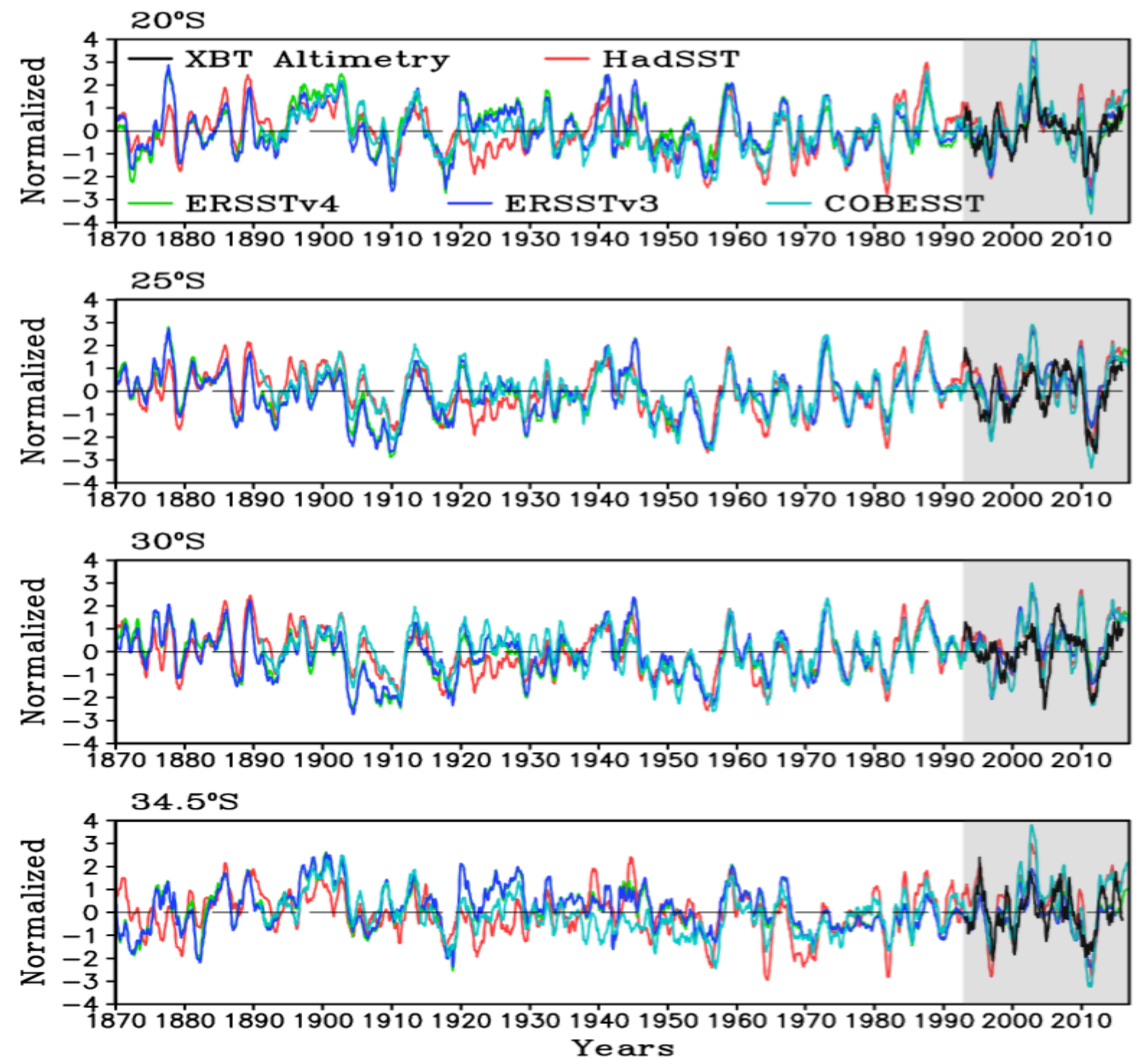

Figure 2. SAMOC time series obtained from altimetry (black) and those reconstructed from four different SST products and SAMOC joint variability (color). All time series were normalized by their standard deviation. The trained period is highlighted by a grey box.

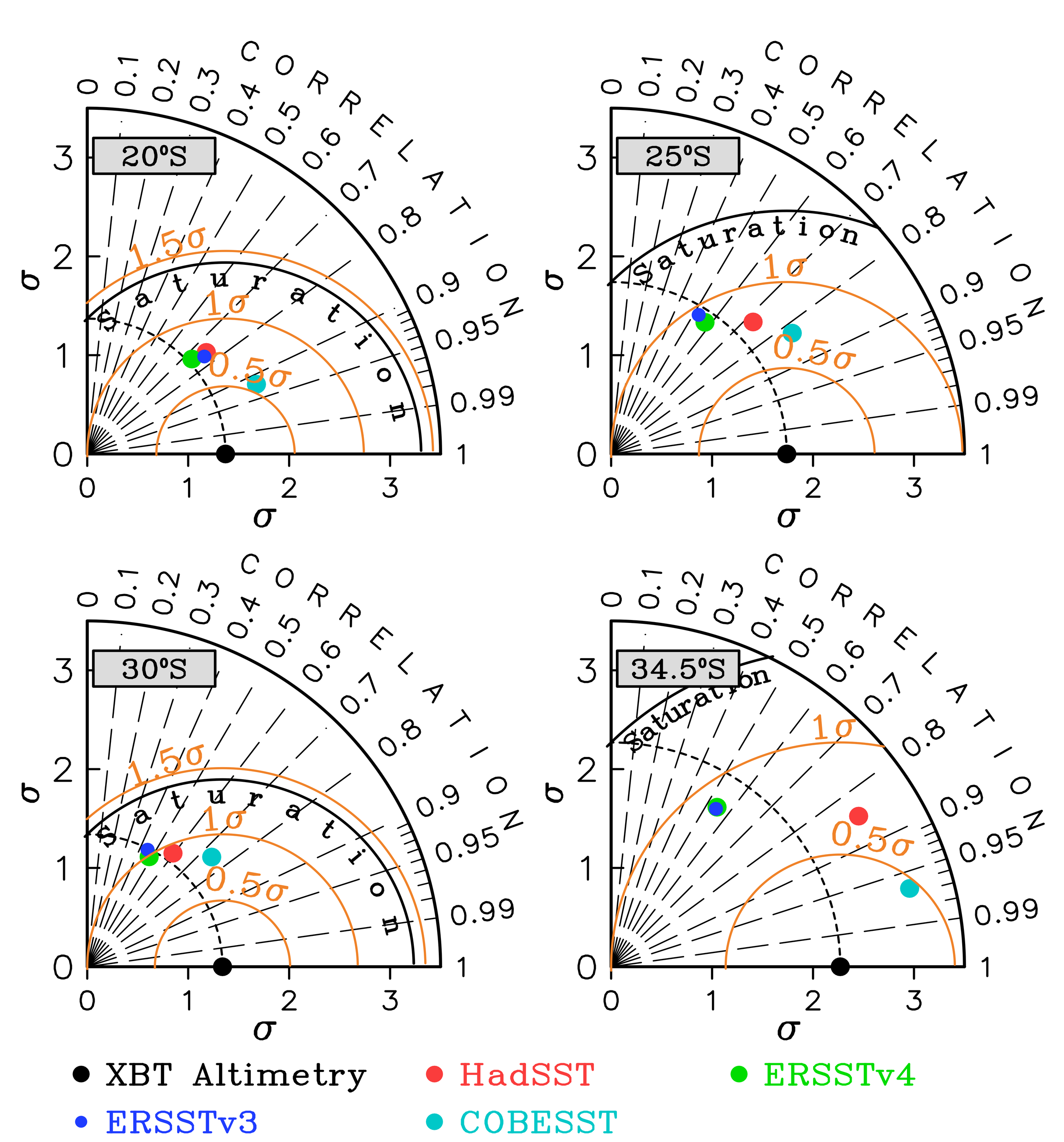

Figure 3. Taylor diagram for the reconstruction of the MOC using different SST products with respect to the observed XBT-altimetry derived MOC (black dot). Note that the radial axes describe standard deviation (σ) in Sverdrup and the azimuthal axis indicates correlation. The concentric orange circles with respect to the observed MOC indicate root-mean-square-error (RMSE) in standard deviation units. That is, the closer a point is to the observed MOC, the better the reconstruction. The RMSE for all reconstructions are significantly smaller than the saturation RMSE (RMSE equal to $\sqrt{2}\sigma$) shown by black semicircle.

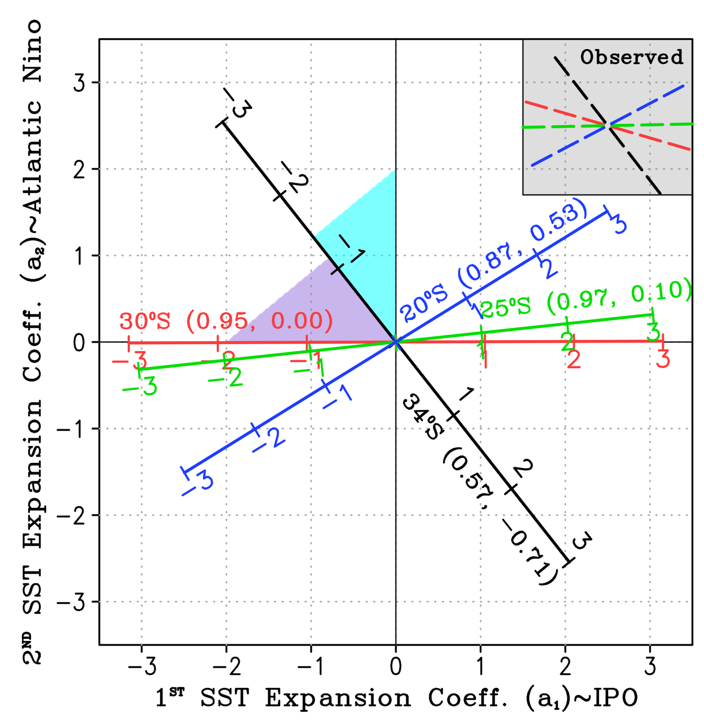

Figure 4. Linear projection between the reconstructed SAMOC at different latitudes (labeled colored axes) and the first two SST expansion coefficients $\boldsymbol{a_1}$ and $\boldsymbol{a_2}$. The projection between any two axes indicates their correlation. The purple (aqua) triangle indicates the projection between $\boldsymbol{a_1}(\boldsymbol{a_2})$ and the AMOC at 34S. The gray rectangle in the upper-right serve to illustrate that the relationship between first two SST expansion coefficients and the observed AMOC at different latitudes is similar.

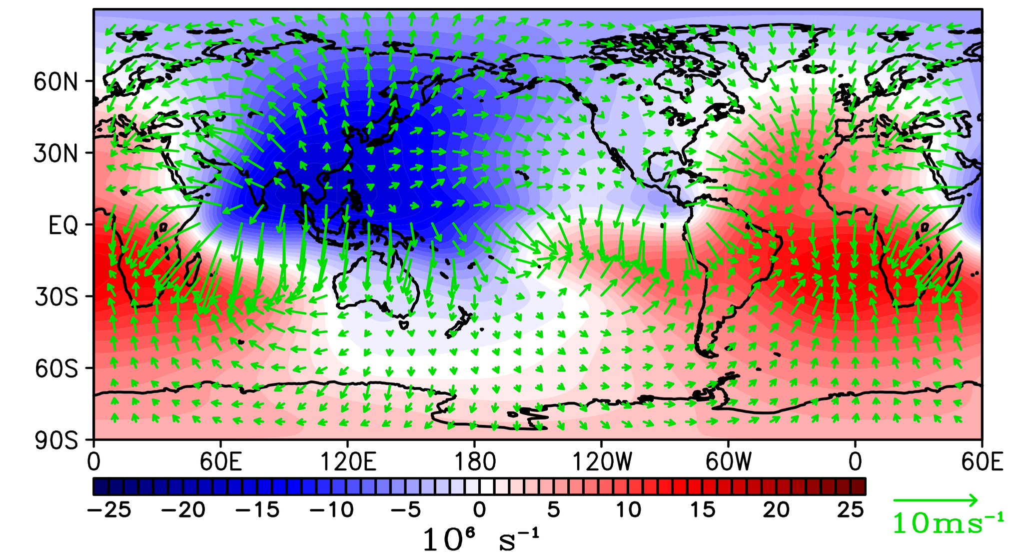

Figure 5. Climatology of boreal summer (June-July-August) 200mb velocity potential and divergent wind component. Enhanced precipitation regions are characterized by negative (blue) velocity potential and divergence wind. Note that the South Atlantic region serves as the main balance for inter-hemispheric atmospheric circulation.

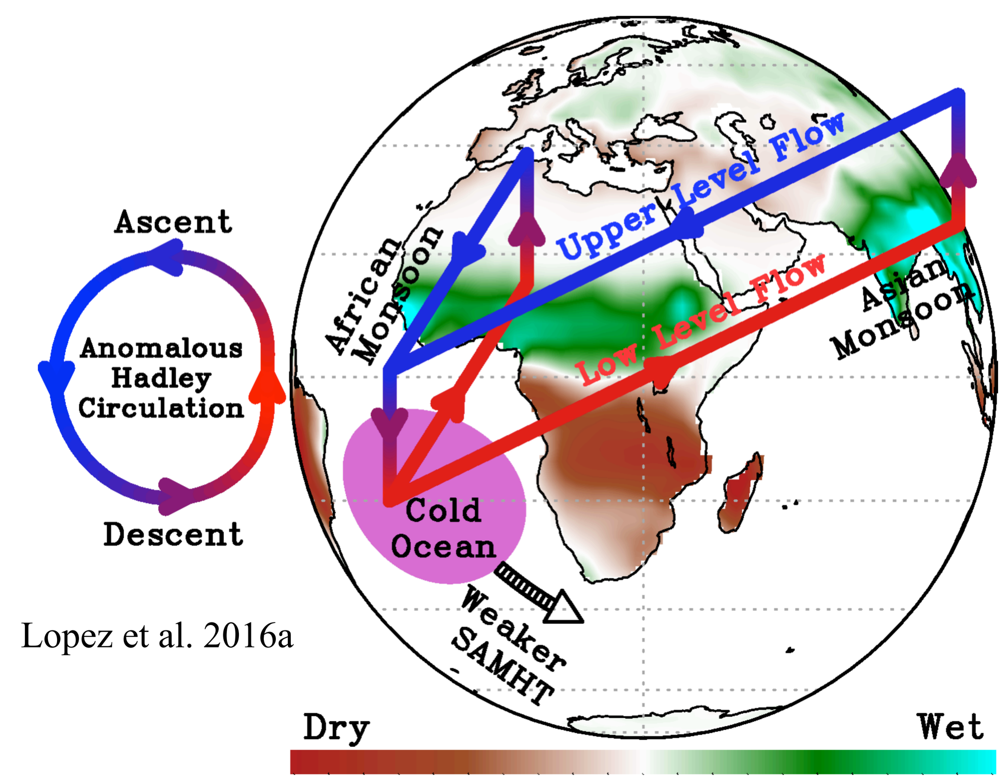

Figure 6. Schematic diagram of the role of weaker-than-normal heat transport (SAMHT) in anomalous atmospheric circulation at 20 years lead-time. Weakened SAMHT is shown by thick black arrows. This results in a cooler than normal South Atlantic Ocean (labeled by purple shade) which produce an anomalous Hadley circulation labeled by counterclockwise circulation. This anomalous Hadley circulation brings moisture to the Northern Hemisphere (NH) and heat towards the Southern Hemisphere (SH). This circulation sense produces ascent and precipitation in the NH thus enhancing the NH monsoons and descent and less precipitation in the Southern Hemisphere.

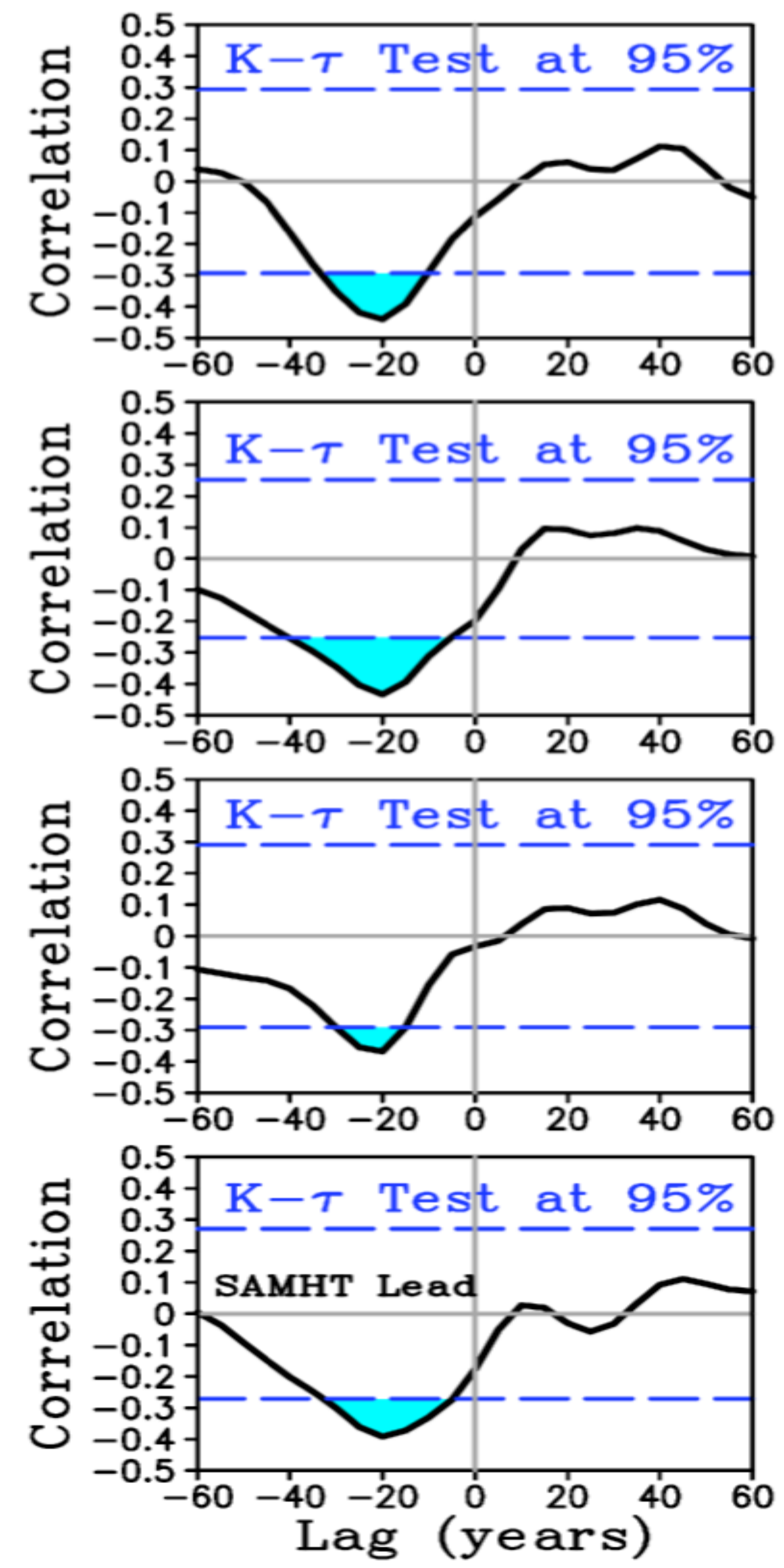

Figure 7. Lag-lead Spearman ranked correlation between SAMHT and NH monsoon indices(i.e., Indian (INDM), East Asian (EAM), North American (NAM), and North African Monsoon (NAF)). The blue dashed lines depict the 95% significance level based on a non-parametric Kendall-τ test. Negative lag indicates periods when SAMHT leads the NH monsoon index. Periods with significant correlation are shaded blue.

Acknowledgement: This research was carried out under the auspices of the Cooperative Institute of Marine and Atmospheric Studies, a cooperative institute of the University of Miami and the National Oceanic and Atmospheric Administration (NOAA), cooperative agreement NA10OAR4320143. This work was supported by NOAA Atlantic Oceanographic and Meteorological Laboratory and funded by the NOAA Climate Program Office.

References:

1. Burgman, R. J., B. P. Kirtman, A. C. Clement, and H. Vazquez, (2017), Model evidence for low-level cloud feedback driving persistent changes in atmospheric circulation and regional hydroclimate. *Geophysical Research Letters*, *44*(1), 428-437.
2. Lee, S. K., W. Park, E. van Sebille, M. O. Baringer, C. Wang, D. B. Enfield, S. G. Yeager, and B. P. Kirtman (2011), What caused the significant increase in Atlantic Ocean heat content since the mid-20th century?, *Geophysical Research Letters*, *38*(17).
3. Lopez H., S. Dong, S-K Lee, and G. Goni (2016a): Decadal modulations of Interhemispheric Global Atmospheric Circulations and Monsoons by the South Atlantic Meridional Overturning Circulation. *J. Climate,* **29**, 1831–1851, doi: 10.1175/JCLI-D-15-0491.1.
4. Lopez, H., S. Dong, S.-K. Lee, and E. Campos (2016b): Remote influence of Interdecadal Pacific Oscillation on the South Atlantic meridional overturning circulation variability, *Geophysical Research Letter.,* 43, 8250–8258.
5. Lopez H., G. Goni, and S. Dong (2017): A reconstructed South Atlantic Meridional Overturning Circulation time series since 1870. *Geophysical Research Letter,* doi: 10.1002/2017GL073227.
6. Talley, L. D. (2003), Shallow, intermediate, and deep overturning components of the global heat budget, *Journal of Physical Oceanography*, *33*(3), 530-560.

Q-R code to Lopez et al. 2017